Cold collisions of SH– with He: Potential energy surface and rate coefficients

C T Bop, T Trabelsi, K. Hammami, M Mogren Al Mogren, F. Lique, M. Hochlaf

Cold collisions of SH⁻ with He: Potential energy surface and rate coefficients

C. T. Bop,[1,a)] T. Trabelsi,[2] K. Hammami,[2] M. Mogren Al Mogren,[3] F. Lique,[4] and M. Hochlaf[5,b)]

[1]*Laboratory of Atoms Lasers, Department of Physics, Faculty of Sciences and Techniques, University Cheikh Anta Diop of Dakar, Dakar, Senegal*
[2]*Laboratory of Atomic Molecular Spectroscopy and Applications, Department of Physics, Faculty of Sciences, University Tunis El Manar, Campus Universities, 1060 Tunis, Tunisia*
[3]*Chemistry Department, Faculty of Science, King Saud University, P.O. Box 2455, Riyadh 11451, Kingdom of Saudi Arabia*
[4]*LOMC-UMR 6294, CNRS-Université du Havre, 25 Rue Philippe Lebon, BP 1123, 76 063 Le Havre Cedex, France*
[5]*Université Paris-Est, Laboratoire Modélisation et Simulation Multi Echelle, MSME UMR 8208 CNRS, 5 Blvd. Descartes, F-77454 Marne-la-Vallée, France*

Collisional energy transfer under cold conditions is of great importance from the fundamental and applicative point of view. Here, we investigate low temperature collisions of the SH⁻ anion with He. We have generated a three-dimensional potential energy surface (PES) for the SH⁻($X^1\Sigma^+$)–He(^{1}S) van der Waals complex. The *ab initio* multi-dimensional interaction PES was computed using the explicitly correlated coupled cluster approach with simple, double, and perturbative triple excitation in conjunction with the augmented-correlation consistent-polarized valence triple zeta Gaussian basis set. The PES presents two minima located at linear geometries. Then, the PES was averaged over the ground vibrational wave function of the SH⁻ molecule and the resulting two-dimensional PES was incorporated into exact quantum mechanical close coupling calculations to study the collisional excitation of SH⁻ by He. We have computed inelastic cross sections among the 11 first rotational levels of SH⁻ for energies up to 2500 cm⁻¹. (De-)excitation rate coefficients were deduced for temperatures ranging from 1 to 300 K by thermally averaging the cross sections. We also performed calculations using the new PES for a fixed internuclear SH⁻ distance. Both sets of results were found to be in reasonable agreement despite differences existing at low temperatures confirming that accurate predictions require the consideration of all internal degrees of freedom in the case of molecular hydrides. The rate coefficients presented here may be useful in interpreting future experimental work on the SH⁻ negative ion colliding with He as those recently done for the OH⁻–He collisional system as well as for possible astrophysical applications in case SH⁻ would be detected in the interstellar medium. *Published by AIP Publishing.* https://doi.org/10.1063/1.4994970

I. INTRODUCTION

Inelastic and reactive collisions between ions and neutral species at low temperatures are of fundamental and applicative interests. In the last decades, a huge amount of development, both theoretical and experimental, was achieved in this field since these collisions allow understanding the fundamental processes taking place in chemistry and physics as recently reviewed.[1]

Inelastic collisions under cold conditions have been the object of numerous studies.[2–4] A particular interest is that molecules can be cooled down through collisions, for example, using experimental techniques such as buffer gas cooling. Such collisions have to be considered using pure quantum approaches since quantum effects are expected to dominate collisional processes at low temperatures.

Despite recent progress, the case of negative molecular ions colliding with neutrals is still challenging.[5] Whereas, there are no major distinctions between cations and anions colliding with neutrals at a large intermonomer separation, the situation is quite different at short ranges, where the non-reactive scattering of anions strongly depends on the distance and the angle of the approach.[5] These effects are related to the interaction potentials at the molecular region, where an anion–neutral complex may be formed. Moreover, negative ions may exhibit facile autodetachment if their electron affinities either isolated or complexed are not large enough. Autodetachment is in competition with inelastic processes that may occur during these collisions.

In a pioneer work, Wester and co-workers carried out experiments where state-to-state inelastic collisions of hydroxyl anions with helium were studied. The challenging character in these experiments resides on the full quantum state control of the anions, which are hard to manipulate at low energy regimes. For the OH⁻–He benchmark system, they deduced absolute de-excitation rate coefficients.[6] The

---

a)Electronic mail: cheikhtidiane.bop@ucad.edu.sn
b)Electronic mail: hochlaf@univ-mlv.fr.

assignments of the observed features were supported by quantum scattering theory calculations. However, the theoretical findings did not match perfectly with the experimental ones showing that more theoretical and experimental studies need to be performed to have a better insight in these processes. Indeed, the corrigendum of Ref. 6 shows that the computed data are smaller than the measured ones.

Cold inelastic collisions are also widely present in astrophysical media such as in the interstellar medium (ISM), where they contribute to the excitation of the interstellar species. Several studies were performed in order to help astronomers in the accurate determination of the molecular content of the ISM.[7]

Most of the detected species are neutrals or positively charged ions. Only few negative ions were recently identified. They correspond to negative carbon chains such as $C_{2n+1}N^-$ ($n = 0$–2)[8–10] and $C_{2n+2}H^-$ ($n = 1$–3).[11–13] They were observed toward the carbon rich star IRC +10216, the Low-Mass Protostar IRAS 04368+2557 in L1527, and the cold dark TMC-1 cloud. The reasons for such a very low number of anions present in the ISM were attributed to their favorable autodetachment via non-adiabatic effects and/or after reactive collisions with surrounding atoms, molecules, and substrates hence forming neutral species.[14]

Here, we are interested in the cold collision implying the SH^- anion and the He atom. The SH^- anion has a large positive electron affinity ($\sim$2.31 eV[15]). It is thus a stable species in the gas phase. Interaction between He and SH^- can also be a good candidate for future scattering experiments such as those performed recently on the OH^-–He system.[6] In addition, its neutral and cation associated species, SH and SH^+, were recently detected in space.[16,17] SH^- can then be a constituent of the ISM and joins the list of S-bearing diatomic molecules that were already detected: CS,[18] SO,[19] NS,[20] SiS,[21] and SO^+.[22] In the case of the detection of SH^-, collisional rate coefficients for the SH^-–He system will be of primary interest for the analysis of the interstellar spectra.

In this paper, we first mapped the SH^-–He interaction potential in the Jacobi coordinates (see Fig. 1). The electronic structure computations were performed using explicitly correlated coupled cluster approach. A full three dimensional
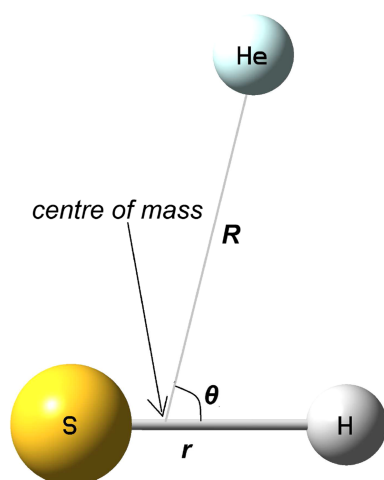
potential energy surface (3D-PES) was generated. Afterwards, the 3D-PES averaged over the ground vibrational wave function of SH^- was incorporated into quantum dynamical calculations to deduce the rotational (de-)excitation cross sections of SH^- colliding with He and the corresponding rate coefficients. The results were compared with those obtained from the same PES but for a fixed internuclear SH^- distance. Hence, we will check on the accuracy of the use of interaction potentials calculated within the rigid rotor (RR) approximation for solely the experimental equilibrium distance of the molecule (i.e., the accuracy of pure 2D-PESs).

The present data should help in interpreting corresponding experimental data whenever measured. As pointed out above, collisional data were rarely measured for negative ions and theoretical computations such as those performed here represent precious help with respect to this objective. Finally, we will carry out a comparison with the OH^-–He isovalent system for which both theoretical and experimental data are available.[6,23]

This paper is organized as follows: Sec. II presents the potential energy surfaces along with the computational details. Section III presents our dynamical computations data and the comparison to the OH^-–He system. In Sec. IV, some concluding remarks are drawn.

II. POTENTIAL ENERGY SURFACE

To compute the SH^-–He interaction potential, preliminary computations were first performed using the complete active space self-consistent field method (CASSCF)[24,25] to check on the monoconfigurational character of the SH^-–He van der Waals system over a large range of internuclear configurations. These computations showed that the dominant electronic configuration of the ground electronic state of the SH^-–He system has a weight greater than 99.50%. Hence, we followed the methodology that we established for the generation of potentials using explicitly correlated calculations. Briefly, the calculations were carried out using the explicitly correlated coupled cluster approach with single, double and perturbative triple excitation CCSD(T)-F12[26] as implemented in the Molpro suite (version 2012).[27] The atoms were described with the augmented-correlation consistent-polarized valence triple zeta (aug-cc-pVTZ) basis set.[28,29] The MOLPRO default choices for the density fitting and resolution of identity basis sets have been applied.[30] As we established,[31–34] this level of theory ensures taking into account large part of electronic correlation similar to that reached by using the standard coupled cluster technique extrapolated to the complete basis set (CBS) limit.

We computed a potential energy surface modeling the interactions between a diatomic anion and a structureless neutral atom. For related studies, the internuclear distance of the diatom is usually kept frozen at its experimental value. Nevertheless, a 3D-PES is more suited if molecules are prepared in a vibrationally excited state, which is of interest to interpret future possible experiments. In addition, it was recently established that an accurate description of the target vibrational motion in the van der Waals complex is needed for low energy scattering.[35] Indeed, there is a need to accurately take into account the vibrational motion of diatomic

FIG. 1. Body–fixed Jacobi coordinates of the SH^-–He collisional complex.

molecules in the construction of potential energy surfaces, especially those implying molecular hydrides where a significant anisotropy with respect to the internuclear distance r is expected.

Therefore, we generated a 3D-PES of SH$^-$ interacting with He. In the calculations, the SH$^-$–He van der Waals system was described with the Jacobi coordinates r, R, and θ: r represents the internuclear distance of SH$^-$, R is the scattering distance (i.e., the distance linking the centre of mass of SH$^-$ and He), and θ stands for the angle that form the two distance vectors (see Fig. 1).

The 3D-PES, V(r, R, θ), was calculated by setting the r-distance to 5 values (2.13, 2.33, 2.53, 2.72, and 2.92 a$_0$) leading to consider the vibrational states of the SH$^-$ negative ion up to the vibrational level $v = 2$. The scattering R-distance was varied from 3.20 to 100 a$_0$ with an irregular step. Typically, we considered 37 R-values (3.2, 3.4, 3.6, 3.84, 4.2, 4.4, 4.6, 4.8, 5.0, 5.2, 5.4, 5.6, 5.8, 6.0, 6.2, 6.4, 6.6, 6.8, 7.0, 7.2, 7.4, 7.6, 7.8, 8.0, 8.4, 8.8, 9.0, 9.5, 10, 14, 18, 20, 25, 30, 40, 50, and 100 a$_0$). The angular Jacobi coordinate θ was spanned with an uniform step size of $10°$ from $0°$ to $180°$. The 3D-PES was constructed in the C_s symmetry group with 3515 *ab initio* energies for non-redundant nuclear configurations. Note that we corrected for the non-size consistency error of the CCSD(T)-F12 approach by subtracting the value of the potential ~ 1.14 cm^{-1} obtained at 100 a$_0$. This ensures a vanishing potential at large intermonomer separations and hence to a correct asymptotic behavior of the interaction potential. In addition, we have corrected the basis set superposition error (BSSE) with the counterpoise procedure of Boys and Bernardi,[36]

$$V(r,R,\theta) = E_{SH^--He}(r,R,\theta) - E_{SH^-}(r,R,\theta) - E_{He}(r,R,\theta), \quad (1)$$

where $E_{SH^--He}(r,R,\theta)$, $E_{SH^-}(r,R,\theta)$, and $E_{He}(r,R,\theta)$ are the total electronic energies of the SH$^-$–He cluster, the SH$^-$ subsystem, and the He subsystem, respectively. These energies are evaluated in the full basis set of the complex.

For dynamical calculations, an analytical expansion of the potentials is required. We have adopted the fitting procedure described by Werner *et al.*[37] for the CN–He complex. Such a procedure leads us to generate the $V(r,R,\theta)$ numerical expansion routine that is implemented later in the dynamical computations code,

$$V(r,R,\theta) = \sum_{n=1}^{N}\sum_{l=1}^{L} A_{ln}(R)d_{0,0}^{l-1}(\cos\theta)(r-r_e)^{n-1}, \quad (2)$$

where $d_{0,0}^{l-1}$ are the reduced rotation matrix elements of Wigner, and L and N represent, respectively, the numbers of the scattering angles and the SH$^-$ internuclear distances. The analytical potential is found to reproduce the calculated surface quite well. The deviations between the fitted potential values and the *ab initio* points are concentrated in the repulsive part of the PES, and the mean difference between the analytical fit and the *ab initio* calculations is $\sim$2%-3%.

The calculated *ab initio* 3D-PES was averaged over the ground vibrational wave function ($v = 0$) of the SH$^-$ molecule. Thus, we have determined the averaged 3D-PES with the following algorithm:

$$V(R,\theta) = \langle \varphi_{v=0}(r) \mid V(r,R,\theta) \mid \varphi_{v'=0}(r)\rangle, \quad (3)$$

$$V(R,\theta) = \sum_{n=1}^{N}\sum_{l=1}^{L} A_{ln}(R)d_{0,0}^{l-1}(\cos\theta) \times M_{0,0}(n), \quad (4)$$

$$M_{v,v'}(n) = \langle \varphi_v(r) \mid (r-r_e)^{n-1} \mid \varphi_{v'}(r)\rangle.$$

The φ_v wave functions were computed using the Fourier Grid Hamiltonian (FGH) program[38,39] from the potential of SH$^-$(X$^1\Sigma^+$) which was calculated with a RKR program[40] using the SH$^-$ experimental constant of Ref. 41. The vibrational wave
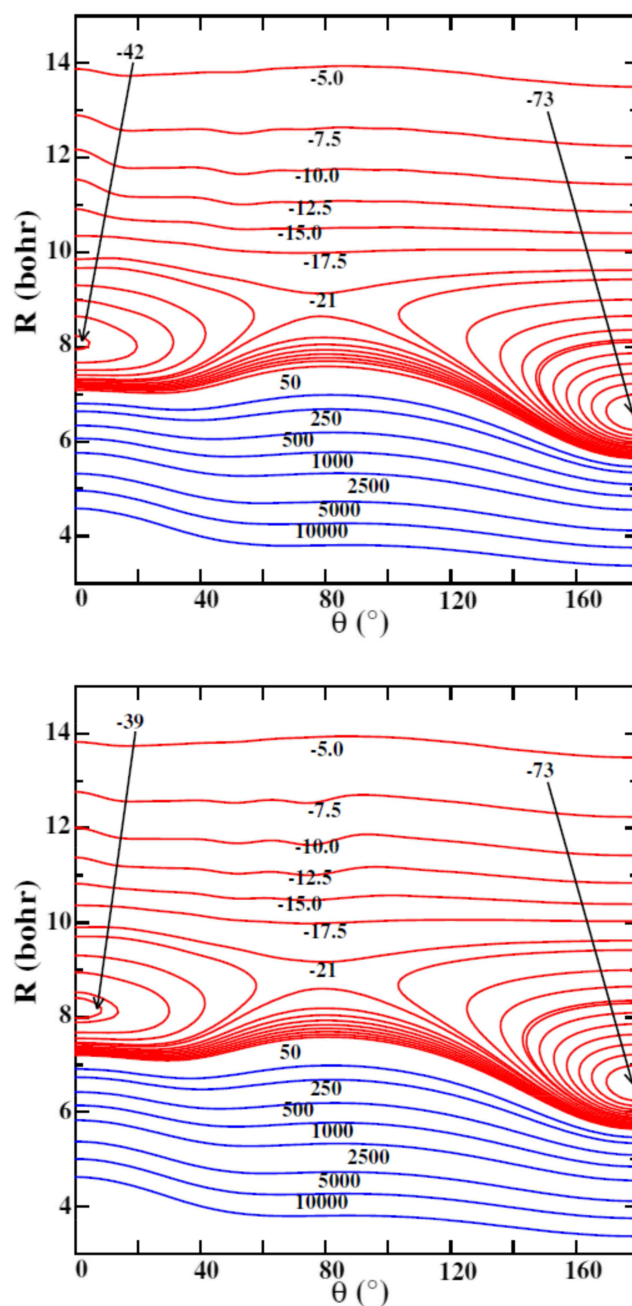

FIG. 2. Contour plots of the SH$^-$–He interaction potentials as a function of the R and θ Jacobi coordinates: the 3D-PES for a fixed r distance of 2.53 bohrs (upper panel) and vibrationally averaged 3D-PES (i.e., av-2D-PES) (lower panel). The blue (red) curves stand for positive (negative) energies (in unit of cm^{-1}). The zero energy is obtained when SH$^-$ and He are separated.

function taken for the rotational state $J = 0$. The resulting PES is denoted hereafter as av-2D-PES.

Figure 2 displays the 3D-PES (upper panel) at a fixed SH$^-$ internuclear distance of $r = 2.53$ bohrs (corresponding to the equilibrium distance of the SH$^-$ molecule) and the av-2D-PES (lower panel). These contour plots of the SH$^-$–He van der Waals system are given as a function of the R and θ Jacobi coordinates. Both interaction potentials are anisotropic and present two minima located at linear configurations (i.e., $\theta = 0°$ and $\theta = 180°$). These two minima are separated by a transition state for θ close to 80°. For av-2D-PES, the deepest potential well occurs at 73.11 cm^{-1} for He approaching toward S (i.e., $\theta = 180°$) and $R = 6.6$ bohrs. The depth of the second minimum is 39.86 cm^{-1} and it is located at R = 8.2 bohrs. The well depths of the 2D-PES at a fixed SH$^-$ internuclear distance are located at almost the same positions. They are however slightly deeper (73.18 cm^{-1} for $\theta = 180°$ and 42.42 cm^{-1} for $\theta = 0°$). One can conclude from this comparison that both potentials present close shapes in the intermediate region of the scattering distance. However, some deviations are observed in the short range part of the PESs, particularly for $\theta = 0°$-10°.

With respect to the OH$^-$–He system, both potentials present two minima in the linear geometries and the deeper one occurs for the He approach toward the heavier atom of the anion (i.e., S for SH$^-$ and O for OH$^-$, see Table I). However, the anisotropies of the two interaction potentials are different since the minimum observed for He approaching toward H (the lighter atom) is deeper for SH$^-$ than that for OH$^-$ (while the other minimum is deeper for OH$^-$).

In 2D and av-2D PESs, the saddle point for the T-shape geometry is −21 cm^{-1} below the He–SH$^-$ PES asymptote. Therefore, large amplitude motions or quantum vibrational localizations for the rovibrational states located above this barrier are expected. Recently, such effects were identified for SH$^-$–N, SN$^-$–H,[42] and NO$^+$–Ar[43] weakly bound complexes. These effects are worth probing by means of experimental setups.

The influence that the difference mentioned above may carry on dynamical calculations will be presented and discussed in Sec. III. To this end, we have implemented the potentials in the MOLSCAT code.[44] Both interaction potentials have been expanded over the Legendre polynomial functions by including terms up to $\lambda_{max} = 18$ such as

$$V(R, \theta) = \sum_{\lambda} V_{\lambda}(R)P_{\lambda}(\cos\theta). \tag{5}$$

The SH$^-$–He PES and the SH$^-$ potential energy curves can be found in the supplementary material.

III. COLLISIONAL DYNAMICS

One of the objectives of the present work is the determination of (de-)excitation cross sections and rate coefficients for the negative ion SH$^-$ in collision with He. All dynamical calculations were carried out with the 3D-PES at a fixed internuclear distance and with the av-2D-PES using the same parameters to probe the impact of the vibration in the magnitude of the collisional data.

A. Rotational cross sections

In this paper, we only consider the pure rotational excitation of SH$^-$ induced by collision with He. The collisional energy range considered in this paper (up to 2500 cm^{-1}) is below the first excited vibrational level of SH$^-$ ($w_e = 2647.07$ cm^{-1})[45] so that vibrational excitation is not likely to occur and can be omitted. Note that the 3D-PES we generated can be used for those purposes if needed.

The excitation cross sections calculations were performed using the quantum mechanical close-coupling (CC) approach of Arthurs and Dalgarno[46] as implemented in the MOLSCAT program. In the following, J denotes the rotational state of the SH$^-$ anion. The total energy range was spanned as follows: for E ≤ 100 cm^{-1}, the step was set to 0.1 cm^{-1}; for 100 ≤ E ≤ 200 cm^{-1}, the step was set to 0.5 cm^{-1}; for 200 ≤ E ≤ 500 cm^{-1}, the step was set to 1 cm^{-1}; for 500 ≤ E ≤ 1000 cm^{-1}, the step was set to 5 cm^{-1}; for 1000 ≤ E ≤ 1500 cm^{-1}, the step was set to 10 cm^{-1}; and for 1500 ≤ E ≤ 2500 cm^{-1}, the step was set to 20 cm^{-1}. The rotational levels of SH$^-$ are obtained from the spectroscopic constants reported in Table II. We have performed some convergence tests to set up the MOLSCAT parameters. The selected parameters are given in Table II. The STEPS integration parameter which is inversely proportional to the integration step was set to 20 for E ≤ 100 cm^{-1} and 10 for the other energy values. The integration limits are set to $R_{min} = 2$ bohrs and $R_{max} = 90$ bohrs. The size of the rotational basis defined by J_{max} was set to 7 for total energy E ≤ 100 cm^{-1} and progressively increased to $J_{max} = 17$ for energy up to 2500 cm^{-1}. In addition, for elastic (inelastic) transitions, the diagonal (off-diagonal) tolerance was set to DTOL = 0.01 Å^2 (OTOL = 0.001 Å^2). This allows setting the limit value of the total angular momentum (J_{tot}) large enough for a best convergence of cross sections. For example, we have obtained $J_{tot} = 157$ at 100 cm^{-1}, $J_{tot} = 236$ at 1000 cm^{-1}, and $J_{tot} = 280$ at 2500 cm^{-1}. Such a high number was needed for convergence of the elastic cross sections. The log derivative method was used to solve the coupled equations.[47]

Figure 3 displays the rotational de-excitation cross sections of SH$^-$ induced by collision with He as a function of

TABLE I. Potential wells (in units of cm^{-1}) of the SH$^-$–He and OH$^-$–He systems. For OH$^-$–He, these values were estimated from Ref. 23.

Geometry	This work		Reference 23
θ (deg)	2D-PES	av-2D-PES	OH$^-$–He
0	42.42	39.86	≥25
180	73.18	73.11	≥100

TABLE II. MOLSCAT parameters used in this work.

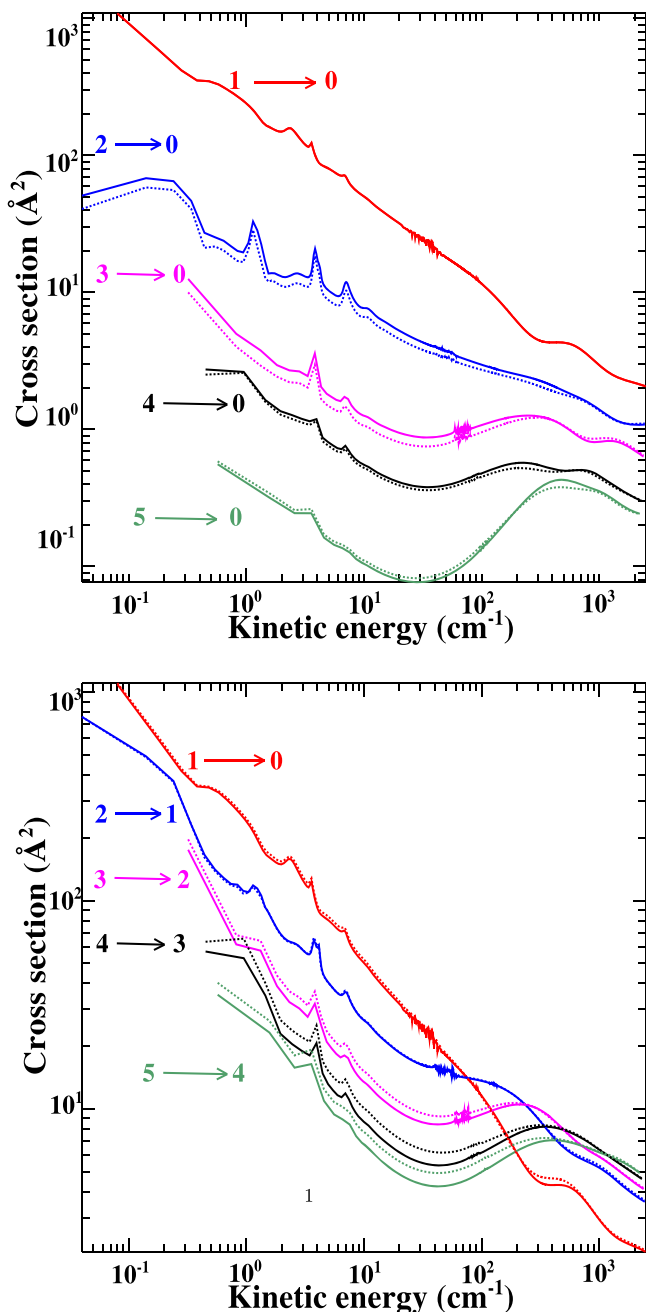|	
STEPS = 20, 10	$J_{max} = 7, 8, 10, 13, 15, 16, 17$
$D_e = 4.984 \times 10^{-4}$ cm^{-1},[45]	$R_{min} = 2\, a_0$
$B_e = 9.562\,53$ cm^{-1},[45]	$R_{max} = 90\, a_0$
DTOL = 0.01 Å^2	OTOL = 0.001 Å^2
$\mu = 3.57$ amu	

FIG. 3. Rotational de-excitation cross sections of SH⁻ induced by collision with He as a function of the kinetic energy for $J \rightarrow 0$ (upper panel) and $\Delta J = 1$ (lower panel) transitions. The dotted lines (solid lines) correspond to cross sections obtained from the vibrationally averaged av-2D (pure two dimensional) PES.

the kinetic energy for $J \rightarrow 0$ (upper panel) and $\Delta J = 1$ (lower panel) transitions. The dotted lines correspond to data obtained from the av-2D-PES and the solid lines correspond to data obtained from the pure 2D-PES. For the $1 \rightarrow 0$ and $2 \rightarrow 1$ transitions, both potentials lead to very close cross section values while deviations are observed in the $2-5 \rightarrow 0$, $3 \rightarrow 2$, $4 \rightarrow 3$, and $5 \rightarrow 4$ transitions. When the collision energy increases, the difference between the two sets of results decreases. These differences reflect a slightly different anisotropy of the two PESs. Such conclusion was already addressed for the OH–He neutral system by Kalugina *et al.*[35] who found that the use of

a vibrationally averaged 3D-PES is desired to investigate the excitation of diatomic hydrides at very low energies. In detail, the differences remain however small, and the pure rotational excitation of SH⁻ induced by collision with He can be reasonably well described by the use of a pure 2D PES. Recently, Faure *et al.*[48] investigated in detail the impact of the vibration of the target on the computation of pure rotational excitation for the CO–H₂ system. These authors found that the use of a rigid rotor PES is reliable when the equilibrium distance is corresponding to the vibrationally averaged distance. For SH⁻, this would correspond to an internuclear distance of 2.57 a_0. Hence, we may expect a better agreement between results obtained from pure 2D and av-2D PESs if the equilibrium distance is 2.57 a_0.

Some resonances can be observed in these cross sections at low energies. This behavior was noted in early studies as well as in the recent ones.[2,49,50] They are of either shape or Feshbach nature. The Feshbach resonances were interpreted as a temporary trapping of helium in the potential well, where the complex (SH⁻–He) forms quasi-bound states and shape resonances correspond to quasi-bound states occurring from tunneling via the centrifugal energy barrier. The fine step size used at energies below 100 cm⁻¹ was crucial for a correct description of these resonances.

Concerning propensity rules, the $1 \rightarrow 0$ transition predominates in the two panels at low collision energies. At higher collision energies, transitions implying highest rotational states start to dominate. From the analysis of these curves, one can conclude that transitions involving $\Delta J = 1$ values outweigh the $\Delta J = 2$ ones. We anticipate that this propensity rule persists in the collisional rates.

B. Rate coefficients

The rate coefficients were computed for temperatures ranging from 1 to 300 K for all energy levels with $J \leq 10$, by thermally averaging the cross sections over a Maxwell–Boltzmann velocity distribution,

$$k_{J \rightarrow J'}(T) = \left(\frac{8}{\pi \mu k_B^3 T^3} \right)^{\frac{1}{2}} \int_0^\infty \sigma_{J \rightarrow J'} \, E_c \, \exp\left(-\frac{E_c}{k_B T}\right) dE_c, \quad (6)$$

where $\sigma_{J \rightarrow J'}$ is the cross section from initial state J to final state J', μ is the SH⁻–He reduced mass, and k_B is Boltzmann's constant.

We present in Fig. 4 the SH⁻ de-excitation rate coefficients induced by collision with He as a function of the kinetic temperature for $J \rightarrow 0$ (upper panel) and $\Delta J = 1$ (lower panel) transitions. The curves obtained using the av-2D-PES are plotted with dotted lines, whereas solid lines represent those computed using the pure 2D-PES for a unique SH⁻ internuclear distance (of 2.53 bohrs). As anticipated, small deviations occur between the two sets of data. At high temperatures, the difference between both PESs is small enough to validate the use of a pure 2D-PES in scattering calculations. The upper panel confirms that the propensity rules are in favor of $\Delta J = 1$ transitions.

Finally, Table III gives the rate coefficients of both isovalent negative ions (SH⁻ and OH⁻) induced by collision with He at low temperatures for comparison. The data obtained
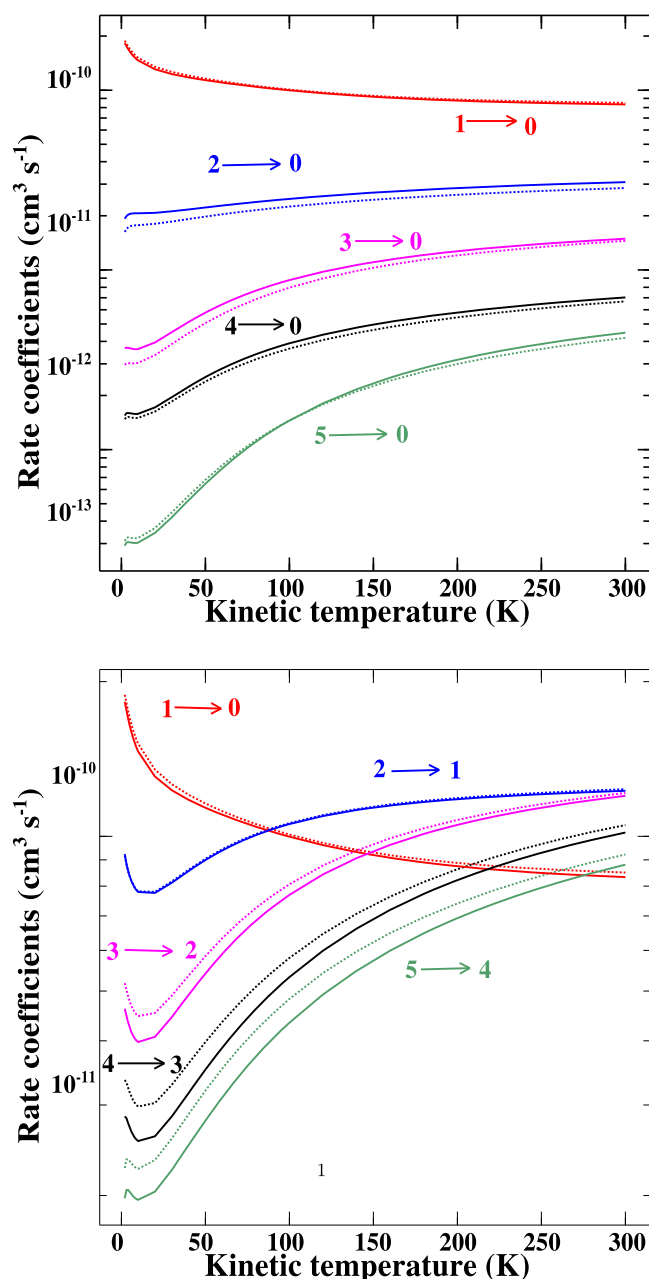
FIG. 4. Rate coefficients of SH$^-$ induced by collision with He as a function of the kinetic temperature for $J \rightarrow 0$ (upper panel) and $\Delta J = 1$ (lower panel) transitions. The dotted lines (solid lines) are obtained using av-2D-PES (the 3D-PES for a fixed r distance of 2.53 bohrs).

in this work for SH$^-$–He system are ~7.4 times greater than those measured for OH$^-$–He.[6] Two main reasons can explain this difference: (i) the smaller energy spacing between SH$^-$ rotational states than that between OH$^-$ rotational states and

TABLE III. Comparison of rotational de-excitation rate coefficients ($\times 10^{-10}$ cm^3 s^{-1}) of the SH$^-$ and OH$^-$ isovalent negative ions induced by collision with He at low temperatures. All data correspond to the $1 \rightarrow 0$ transition. The SH$^-$ data are those obtained from the av-2D PES.

T (K)	k_{SH^-}	k_{OH^-}	k_{SH^-}/k_{OH^-}
22	1.328	0.180[a]	7.378

[a]Refer to data of Hauser *et al.*[6]

(ii) the different anisotropy of the PESs of the two systems. Hence, we expect that experiments on the SH$^-$–He system could also lead to the accurate measurement of the rotational rate coefficients at low temperatures because of a possible strong signal.

IV. CONCLUSION

We have computed a multi-dimensional PES for the SH$^-$–He van der Waals system at the CCSD(T)-F12/aug-cc-pVTZ level of theory. The PESs were incorporated into quantum mechanical computations to deduce the state-to-state rotational (de-)excitation cross sections of SH$^-$ by He. These cross sections are obtained for total energies up 2500 cm^{-1}. Using a Maxwell–Boltzmann velocity distribution, we have thermally averaged these cross sections and obtained rate coefficients for temperatures ranging from 1 to 300 K.

In this work, we note that the pure two-dimensional potential is well suited to deduce the rotational cross sections and rate coefficients. Indeed, our results show that the SH$^-$ vibrational motion does have not a major effect on the scattering process. However, slight deviations occur at low temperatures between the two sets of results obtained with pure two-dimensional and av-2D PESs. This difference may be seen in future highly accurate experimental studies.

Concerning propensity rules, the $\Delta J = 1$ transitions are favored compared to the $\Delta J = 2$ ones. It is expected that the data computed in this paper may be of great interest for future experimental studies as well as the interstellar detection of the SH$^-$ negative ion.

SUPPLEMENTARY MATERIAL

See supplementary material for the analytical forms of the SH$^-$–He potential energy surface and the SH$^-$ potential energy curves.

ACKNOWLEDGMENTS

[1]D. Zhang and S. Willitsch, preprint arXiv:1703.07133 (2017).
[2]S. Chefdeville, Y. Kalugina, S. Y. van de Meerakker, C. Naulin, F. Lique, and M. Costes, Science **341**, 1094 (2013).
[3]A. Bergeat, J. Onvlee, C. Naulin, A. van der Avoird, and M. Costes, Nat. Chem. **7**, 349 (2015).
[4]J. Jankunas, K. Jachymski, M. Hapka, and A. Osterwalder, "Communication: Importance of rotationally inelastic processes in low-energy penning ionization of CHF$_3$," J. Chem. Phys. **144**, 221102 (2016).
[5]J. Mikosch, M. Weidemüller, and R. Wester, Int. Rev. Phys. Chem. **29**, 589 (2010).
[6]D. Hauser, S. Lee, F. Carelli, S. Spieler, O. Lakhmanskaya, E. S. Endres, S. S. Kumar, F. Gianturco, and R. Wester, Nat. Phys. **11**, 467 (2015).

[7] E. Roueff and F. Lique, Chem. Rev. **113**, 8906 (2013).

[8] M. Agúndez, J. Cernicharo, M. Guélin, C. Kahane, E. Roueff, J. Kłos, F. Aoiz, F. Lique, N. Marcelino, J. Goicoechea *et al.*, Astron. Astrophys. **517**, L2 (2010).

[9] P. Thaddeus, C. Gottlieb, H. Gupta, S. Brünken, M. McCarthy, M. Agúndez, M. Guélin, and J. Cernicharo, Astrophys. J. **677**, 1132 (2008).

[10] J. Cernicharo, M. Guélin, M. Agúndez, M. McCarthy, and P. Thaddeus, Astrophys. J., Lett. **688**, L83 (2008).

[11] J. Cernicharo, M. Guélin, M. Agúndez, K. Kawaguchi, M. McCarthy, and P. Thaddeus, Astron. Astrophys. **467**, L37 (2007).

[12] H. Gupta, C. Gottlieb, M. McCarthy, and P. Thaddeus, Astrophys. J. **691**, 1494 (2009).

[13] S. Brünken, H. Gupta, C. Gottlieb, M. McCarthy, and P. Thaddeus, Astrophys. J., Lett. **664**, L43 (2007).

[14] M. Senent and M. Hochlaf, Astrophys. J. **768**, 59 (2013).

[15] W. Chaibi, C. Delsart, C. Drag, and C. Blondel, J. Mol. Spectrosc. **239**, 11 (2006).

[16] D. Neufeld, E. Falgarone, M. Gerin, B. Godard, E. Herbst, G. P. des Forêts, A. Vasyunin, R. Güsten, H. Wiesemeyer, and O. Ricken, Astron. Astrophys. **542**, L6 (2012).

[17] K. M. Menten, F. Wyrowski, A. Belloche, R. Güsten, L. Dedes, and H. S. P. Müller, Astron. Astrophys. **525**, A77 (2011); e-print arXiv:1009.2825.

[18] A. A. Penzias, P. M. Solomon, R. W. Wilson, and K. B. Jefferts, Astrophys. J., Lett. **168**, L53 (1971).

[19] C. A. Gottlieb and J. A. Ball, Astrophys. J., Lett. **184**, L59 (1973).

[20] C. A. Gottlieb, J. A. Ball, E. W. Gottlieb, C. J. Lada, and H. Penfield, Astrophys. J., Lett. **200**, L147 (1975).

[21] M. Morris, W. Gilmore, P. Palmer, B. E. Turner, and B. Zuckerman, Astrophys. J., Lett. **199**, L47 (1975).

[22] B. E. Turner, Astrophys. J., Lett. **396**, L107 (1992).

[23] L. Gonzalez-Sanchez, F. Marinetti, E. Bodo, and F. Gianturco, J. Phys. B: At., Mol. Opt. Phys. **39**, S1203 (2006).

[24] H.-J. Werner and P. J. Knowles, J. Chem. Phys. **82**, 5053 (1985).

[25] P. J. Knowles and H.-J. Werner, Chem. Phys. Lett. **115**, 259 (1985).

[26] G. Knizia, T. B. Adler, and H.-J. Werner, J. Chem. Phys. **130**, 054104 (2009).

[27] H. Werner, P. Knowles, G. Knizia, F. Manby, M. Schtz, P. Celani, T. Korona, R. Lindh, A. Mitrushenkov, G. Rauhut *et al.*, MOLPRO, version 2012.1, a package of *ab initio* programs, 2012, see http://www.molpro.net.

[28] R. A. Kendall, T. H. Dunning, Jr., and R. J. Harrison, J. Chem. Phys. **96**, 6796 (1992).

[29] T. H. Dunning, Jr., J. Chem. Phys. **90**, 1007 (1989).

[30] K. E. Yousaf and K. A. Peterson, J. Chem. Phys. **129**, 184108 (2008).

[31] F. Lique, J. Kłos, and M. Hochlaf, Phys. Chem. Chem. Phys. **12**, 15672 (2010).

[32] P. Halvick, T. Stoecklin, F. Lique, and M. Hochlaf, J. Chem. Phys. **135**, 044312 (2011).

[33] Y. N. Kalugina, I. A. Buryak, Y. Ajili, A. A. Vigasin, N. E. Jaidane, and M. Hochlaf, J. Chem. Phys. **140**, 234310 (2014).

[34] Y. Ajili, K. Hammami, N. E. Jaidane, M. Lanza, Y. N. Kalugina, F. Lique, and M. Hochlaf, Phys. Chem. Chem. Phys. **15**, 10062 (2013).

[35] Y. Kalugina, F. Lique, and S. Marinakis, Phys. Chem. Chem. Phys. **16**, 13500 (2014).

[36] S. F. Boys and F. Bernardi, Mol. Phys. **19**, 553 (1970).

[37] H.-J. Werner, B. Follmeg, and M. H. Alexander, J. Chem. Phys. **89**, 3139 (1988).

[38] G. G. Balint-Kurti, R. N. Dixon, and C. C. Marston, Int. Rev. Phys. Chem. **11**, 317 (1992).

[39] C. C. Marston and G. G. Balint-Kurti, J. Chem. Phys. **91**, 3571 (1989).

[40] R. LeRoy, University of Waterloo Chemical Physics Research Report CP-657R, 2004.

[41] M. Elhanine, R. Farrenq, G. Guelachvili, and M. Morillon-Chapey, J. Mol. Spectrosc. **129**, 240 (1988).

[42] Y. Ajili, T. Trabelsi, O. Denis-Alpizar, T. Stoecklin, A. Császár, M. M. Al-Mogren, J. Francisco, and M. Hochlaf, Phys. Rev. A **93**, 052514 (2016).

[43] D. Papp, J. Sarka, T. Szidarovszky, A. G. Császár, E. Mátyus, M. Hochlaf, and T. Stoecklin, Phys. Chem. Chem. Phys. **19**, 8152 (2017).

[44] J. Hutson and S. Green, Collaborative computational project, 1994.

[45] M. Gruebele, M. Polak, and R. J. Saykally, J. Chem. Phys. **86**, 1698 (1987).

[46] A. Arthurs and A. Dalgarno, Proc. R. Soc. A **256**, 540–551 (1960).

[47] D. Manolopoulos, J. Chem. Phys. **85**, 6425 (1986).

[48] A. Faure, P. Jankowski, T. Stoecklin, and K. Szalewicz, Sci. Rep. **6**, 28449 (2016).

[49] K. M. Christoffel and J. M. Bowman, J. Chem. Phys. **78**, 3952 (1983).

[50] L. N. Smith, D. J. Malik, and D. Secrest, J. Chem. Phys. **71**, 4502 (1979).